RMetS

ROYAL METEOROLOGICAL SOCIETY

Effects of irrigation and vegetation activity on early Indian summer monsoon variability

Eungul Lee,[a,c,f]* Thomas N. Chase,[a,d] Balaji Rajagopalan,[a,d] Roger G. Barry,[a,b,c]
Trent W. Biggs[e] and Peter J. Lawrence[a]

[a] *Cooperative Institute for Research in Environmental Sciences (CIRES), University of Colorado, Boulder, Colorado, USA*
[b] *National Snow and Ice Data Center (NSIDC) and World Data Center (WDC) for Glaciology, University of Colorado, Boulder, Colorado, USA*
[c] *Department of Geography, University of Colorado, Boulder, Colorado, USA*
[d] *Department of Civil, Environmental, and Architectural Engineering, University of Colorado, Boulder, Colorado, USA*
[e] *Department of Geography, San Diego State University, San Diego, CA, USA*
[f] *Center for Sustainability and the Global Environment (SAGE), University of Wisconsin, Madison, Wisconsin, USA*

ABSTRACT: We examined the effects of land cover change over the Indian subcontinent during pre-monsoon season (March, April, and May – MAM) on early Indian summer monsoon (ISM) rainfall using observed Normalized Difference Vegetation Index (NDVI) and July precipitation for the period of 1982–2003. MAM NDVI anomalies have increased in the Indian subcontinent and the increases are significantly correlated with increases in the irrigated area, not preceding rainfall. July rainfall significantly decreased in central and southern India, and the decrease is statistically related to the increase in the preceding MAM NDVI anomalies. Decreased July surface temperature in the Indian subcontinent (an expected result of increased evapotranspiration due to irrigation and increased vegetation) leads to a reduced land–sea thermal contrast, which is one of the factors driving the monsoon, and therefore weakens the monsoon circulation. A weak early ISM appears to be at least partially a result of irrigation and the resultant increased vegetation and crop activity prior to the monsoon. Copyright © 2008 Royal Meteorological Society

1. Introduction

India is one of the most intensively irrigated regions of the world (Shiklomanov, 1997), and irrigation withdrawals represent 80–90% of all water use (Douglas *et al.*, 2006). Several model studies have analysed the impacts of land use changes on regional climate, especially in the United States (e.g. Chase *et al.*, 1999) and India (e.g. Sud and Fennessy, 1982, 1984; Sud and Smith, 1985; Lohar and Pal, 1995; de Rosnay *et al.*, 2003; Douglas *et al.*, 2006). Early modelling investigations suggested that major modifications of the biosphere in the Indian subcontinent influences monsoon circulation and rainfall by altering the surface energy balance, the planetary boundary layer motion fields, moisture convergence, and the hydrological cycle, and also suggested that the Indian monsoon was significantly weakened by both an increase in surface albedo and by a reduction in surface roughness (e.g. Sud and Smith, 1985). More recent modelling studies suggest that irrigation alters water and energy fluxes on the subcontinental scale in India. For example, de Rosnay *et al.* (2003) conducted

2-year model simulations, directed by the 1987–1988 International Satellite Land Surface Climatology Project datasets, with and without irrigation over the Indian subcontinent. They pointed out that irrigation is a major component of the regional hydrological cycle, affecting in particular the partitioning of net radiation into sensible and latent heat fluxes. Douglas *et al.* (2006) investigated the changes across India in vapour and energy fluxes between a pre-agricultural and a contemporary agricultural land cover. Mean annual vapour fluxes increased by 17% (340 km^3) with a 7% increase (117 km^3) in the monsoon and early post-monsoon (July–December) and a 55% increase (223 km^3) in the late post-monsoon and pre-monsoon (January–May), indicating a dramatic influence of dry-season agriculture on atmospheric moisture and energy fluxes. Lohar and Pal (1995) showed the effect of irrigation on pre-monsoon precipitation over southwest Bengal (22.2 °N, 87.3 °E) for a period of 20 years (1973–1992). In their model simulations, the increase in soil moisture and evapotranspiration as a result of irrigation hinders the development and intensity of sea-breeze circulations and, therefore, leads to diminished pre-monsoon rainfall. In addition to model simulations, observations have also shown the weakening of the global summer monsoon precipitation over the last 56 years (e.g. Wang and Ding, 2006), but the relationship between

* Correspondence to: Eungul Lee, Center for Sustainability and the Global Environment (SAGE), University of Wisconsin, 1710 University Ave., Madison, WI 53726-4087, USA.
E-mail: elee43@wisc.edu; eungul.lee@gmail.com

these changes and land use/land cover has not been established. Using monthly Normalized Difference Vegetation Index (NDVI) data for 18 years (1982–2000) Sarkar and Kafatos (2004) showed that Indian monsoon rainfall and land surface temperature over the Indian subcontinent have a significant impact on the spatial and temporal distribution of vegetation. While the climate affects terrestrial ecosystems, terrestrial ecosystems can also affect the climate by impacting net radiation and surface heat fluxes (e.g. Chase *et al.*, 2000; Pielke *et al.*, 2002; Foley *et al.*, 2003; Lawrence and Chase, In press).

While these model simulations indicate the importance of irrigation, no observational support for these model results has been reported. Irrigated area has increased rapidly in recent decades, a period for which good observational climate datasets are available. The goal of this study is to identify the effects of irrigation/vegetation activity in the observational record through statistical methods. We examine the effects of land cover change over the Indian region (5–30°N and 70–90 °E) on the Indian summer monsoon (ISM), and address the following questions: (1) Are there significant recent changes (for 22 years; 1982–2003) in land use/land cover (irrigation/vegetation activity) over the Indian subcontinent during the pre-ISM season (March, April, and May – MAM), and (2) Can changes in early ISM rainfall be related to changes in land use/land cover?

2. Data and methodology

2.1. Data

NDVI is the unitless difference between near-infrared (channel 2) and red (channel 1) spectral reflectance normalized by their sum (Tucker *et al.*, 2005).

It is calculated as follows:

$$NDVI = \frac{\text{channel 2} - \text{channel 1}}{\text{channel 2} + \text{channel 1}} \quad (1)$$

Spectral vegetation indices are highly correlated with the photosynthetically active biomass, chlorophyll abundance, and energy absorption (e.g. Justice *et al.*, 1985; Myneni *et al.*, 1995), so NDVI can be used as a measure of green leaf density. NDVI also correlates with physical climate variables including rainfall, temperature, and evapotranspiration in a wide range of environmental conditions (e.g. Gray and Tapley, 1985; *Cihlar et al.*, 1991; Sarkar and Kafatos, 2004). The interannual and interseasonal variability of NDVI have been studied for different regions in Africa (Anyamba and Eastman, 1996), India (Sarkar and Kafatos, 2004), North America (Li and Kafatos, 2000), and the southwestern United States (Leavitt *et al.*, in press), whereas others have found global associations of NDVI anomaly patterns (Kawabata *et al.*, 2001; Ichii *et al.*, 2002). We use NDVI as an index for land cover and irrigation development. NDVI and its temporal distribution is a strong predictor of irrigated areas in southern India, with the largest difference between natural and irrigated systems

in the pre-monsoon dry season (December–May) (Biggs *et al.*, 2006). We use NDVI data from the Global Inventory Modelling and Mapping Studies (GIMMS) from the Global Land Cover Facility at the University of Maryland (Tucker *et al.*, 2005). The data were downloaded from the IRI/LDEO Climate Data Library in the International Research Institute for Climate and Society (http://iridl.ldeo.columbia.edu/expert/SOURCES/.UMD/.GLCF/.GIMMS/.NDVIg/.global/ndvi/streamrescale/-999/setmissing_value/dods). The GIMMS NDVI dataset is available from July 1981 through December 2003, so we examine 22 years, from 1982 to 2003. The dataset is derived from imagery obtained from the different advanced very high resolution radiometer instruments on the different National Oceanic and Atmospheric Administration (NOAA) polar-orbiting meteorological satellites NOAA-7, 9, 11, 14, and 16. The NDVI data has a spatial resolution of $0.073° \times 0.073°$, which we aggregated to 1° for the analysis. The data has been corrected for instrument calibration, view geometry, volcanic aerosols, and other effects not related to vegetation change (Tucker *et al.*, 2005). It is also consistent and quantitatively compatible with the new generation global land surface satellite sensor data available from SPOT-4's vegetation instrument (May 1998 to present) and NASA's moderate resolution imaging spectrometers on the terra and aqua platforms (January 2000 to present, and December 2002 to present, respectively) (Tucker *et al.*, 2005).

The NDVI time series are compared with irrigated area reported in census statistics to establish that changes in NDVI indicate irrigation rather than vegetation changes related to interannual variability in precipitation. Annual irrigated area data for India (km^2) are compiled from reports of the Ministry of Agriculture, Government of India (Government of India, 1981–2003) and the Center for Monitoring Indian Economy (CMIE, 2006). Observed precipitation (mm/day) from the Global Precipitation Climatology Project version 2 (GPCP) (Adler *et al.*, 2003) is used to calculate July ISM rainfall, the month of maximum monsoon intensity. The GPCP data is estimated from low-orbit satellite microwave data, geosynchronous-orbit satellite infrared data, and surface rain gauge observations. In order to determine the influence of land cover change during the pre-monsoon season on dynamic atmospheric conditions during the early summer, we use wind vector (m/s) and divergence (s^{-1}) calculated with mean 200 and 850 hPa u- and v-winds (m/s) from the National Centers for Environmental Prediction–National Center for Atmospheric Research (NCEP–NCAR) reanalysis (Kalnay *et al.*, 1996). To examine physical mechanisms linking land cover change to monsoon circulation, we use surface sensible heat flux [SHF (W/m^2)] and latent heat flux [LHF (W/m^2)] from NCEP–Department of Energy (DOE) Atmospheric Model Inter-comparison Project (AMIP-II) reanalysis (Kanamitsu *et al.*, 2002), and observed surface temperature trends from the Goddard Institute for Space Studies (GISS) (http://data.giss.nasa.gov/gistemp/maps/). The

winds from reanalyses are strongly constrained by observational data, but point observations of surface fluxes are unavailable for our domain, so surface heat fluxes are derived solely from the reanalysis model forced by the data assimilation to remain close to observed atmospheric fields (Kalnay *et al.*, 1996). Surface flux data from NCEP–DOE AMIP-II have been used previously for large-scale climatic studies of Asia (e.g. Tomita *et al.*, 2007). We use the dataset with the limitation that surface heat fluxes are heavily influenced by model calculations to assess the consistency with observed surface temperature. Firmly establishing the vegetation–rainfall connection will require more detailed future measurements of surface heat fluxes calculated from observational datasets.

Spatial resolutions (longitude × latitude) of these datasets are $1° × 1°$ for NDVI (converted from $0.073° × 0.073°$), $2.5° × 2.5°$ for GPCP, NCEP–NCAR and NCEP–DOE AMIP-II data, and $2° × 2°$ for GISS surface temperature trend. For GISS temperature data, we use a 250-km smoothing radius, which represents the distance over which a station influences regional temperature estimation. The records for a given location are combined into a single time series, and the resulting dataset is used to estimate regional temperature change on a grid with $2° × 2°$ resolution. Stations located within 250 km of a grid point are used to compute a weighted mean series for that grid point, where the weight decreases linearly to zero at 250 km. As a final step, all station records within 250 km of a given grid point were averaged (Hansen and Lebedeff, 1987; Hansen *et al.*, 1999). The spatial resolutions of these data are suitable for examining the Indian monsoon and have been used in previous studies of monsoons, both in India and elsewhere (e.g. Wang *et al.*, 2000; Chase *et al.*, 2003; Lee *et al.*, 2008). For example, the Indian monsoon region (i.e. $5–30°N$ and $70–90°E$) has 99 grid points in the reanalysis data. Seasonally averaged values during MAM are defined as the pre-ISM season, and July as the month of maximum ISM rainfall. Maximum rainfall occurs in July accounting for about one-third of all ISM rainfall for June, July, August, and September based on data for 1982–2003.

2.2. Statistical methods

In order to derive the dominant pattern of variability from a time series of fields of NDVI, we use empirical orthogonal function (EOF) analysis. Sarkar and Kafatos (2004) used EOFs of NDVI over the Indian subcontinent and the corresponding normalized principal components (PCs) to examine the variability of vegetation in India and its relation to different meteorological parameters. We compute the eigenvectors (i.e. EOFs) of the covariance matrix of MAM NDVI anomalies (deviations from their 1982–2003 means), and the corresponding time series (i.e. PCs) are obtained by the projection of the original data onto the EOFs. At least 70% of data shall exist at each grid point to be included in the EOF analysis over a specified region ($5–30°N$ and $70–90°E$) for the period of 1982–2003. The NDVI data at each

grid cell are multiplied by area-weight of $\sqrt{\cos(\text{latitude})}$ (http://www.atmos.ucla.edu/~munnich/grads/EOF/index.html). The square root in the weighting is used only for EOF analysis (see the supporting online material of von Storch *et al.*, 2004). The standardized PC is defined as the PC time series multiplied by the area-averaged first eigenvalue over the Indian subcontinent, divided by its standard deviation. The first leading EOF (EOF 1) and its corresponding standardized PC 1 of MAM NDVI anomalies are used to examine land cover change in the Indian subcontinent and to calculate the index of land cover change, because EOF 1 is the most powerful single pattern representing the variance of variable (von Storch and Zwiers, 2001).

We examine the spatial distributions of regression trends of NDVI, rainfall, LHF, SHF, and surface temperature with time. To determine the effects of the preceding MAM vegetation activity in India on early ISM variability, we calculate correlation coefficients of the standardized PC 1 of MAM NDVI anomalies with July ISM rainfall anomalies in each grid over India (i.e. $5–30°N$ and $70–100°E$). For robust regression and correlation analyses, we use a non-parametric technique based on the Kendall and Spearman's methods (e.g. Grantz *et al.*, 2007). In order to check the consistency of the relationship between the MAM NDVI and early ISM rainfall with that between the MAM NDVI and atmospheric conditions in July, we use the composite analysis of 200 hPa wind vector, and 200 and 850 hPa divergences for the 5 highest (1998, 1999, 2000, 2001, and 2002) and the 5 lowest (1982, 1983, 1985, 1987, and 1989) years of the standardized PC 1 of MAM NDVI anomalies over the Indian subcontinent. Composite differences in wind vector and divergences are calculated by subtracting the mean values for the 5 lowest years of MAM NDVI PC 1 from those for the 5 highest years.

3. Changes in land use/land cover: irrigation and NDVI

Figure 1(a) represents the percentage of 5-min grid cell area that was equipped for irrigation and shows large regions where irrigated areas exceed 90% of the total land area. Most Indian rainfall occurs during the monsoon season (June–September), while the rest of the year is dry. As part of the green revolution in the last few decades, numerous irrigation structures were built and the expansion of groundwater pumping has helped increase the irrigated area enormously. Figure 1(b) shows recent upward trends in net irrigated area for India. The spatial distributions of EOF 1 of MAM NDVI anomalies show positive eigenvalues over the entire Indian subcontinent with higher values in the central-western and north-eastern regions (Figure 1(c)). The EOF 1 accounts for 24% of the total variance. The time series of the corresponding standardized PC 1 for 1982–2003 shows a positive trend (Figure 1(d)). The results of our EOF analysis are consistent with the work of Sarkar and
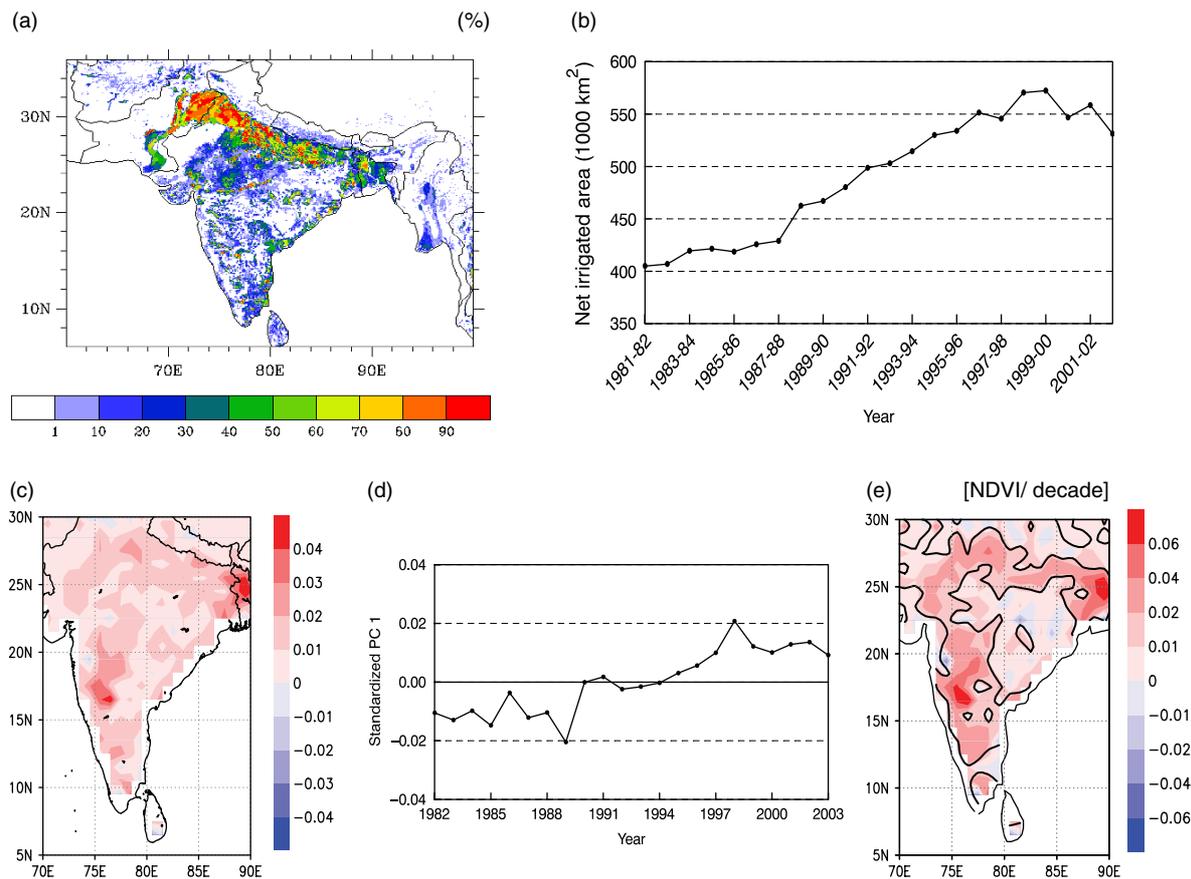
Figure 1. (a) Percentage of land surface equipped for irrigation (Siebert *et al.*, 2005). (b) Time series of net irrigated area for India for 1982–2003. The EOF 1 (23.98% variance) (c) and the corresponding standardized PC time series (d) of MAM NDVI anomalies for 1982–2003 over India, i.e. 5–30°N and 70–90°E. Anomalies are area-weighted values. (e) Spatial distribution of 1982–2003 regression trend of the MAM NDVI (NDVI/decade). Significant regions at the 90% level are contoured. This figure is available in colour online at www.interscience.wiley.com/ijoc

Kafatos (2004), who showed positive eigenvalues in the spatial pattern of EOF 1 of monthly NDVIs over South Asia (0–40°N and 40–100°E) for 1982–2000, and a positive trend in its corresponding PC 1 time series. They are also consistent with the 1982–2003 regression trend of the MAM NDVI, which shows significant increases in the central and northern regions (Figure 1(e)). There has been a strong increase in the MAM NDVI in the eastern region of the Western Ghats around 17°N and 77°E with an increment of 0.02–0.06 NDVI per decade. Both detailed satellite-based change detection and ground truth showed that this increase in NDVI is due to irrigation expansion (Thenkabail *et al.*, 2007). It is an interesting trend, because July ISM rainfall has been decreasing significantly in the same region for the same period (Figure 2(a)). This result suggests a plausible relationship between increased irrigation and vegetation activity and decreased July ISM rainfall, which will be explained in Sections 4 and 5.

The standardized PC 1 of MAM NDVI anomalies (Figure 1(d)) are significantly and positively correlated with the net irrigated area (Figure 1(b)) (Pearson's $r = 0.87$, *p-value* < 0.01). Kendall and Spearman's correlations are consistent with the Pearson's correlation value ($r = 0.69$ for Kendall and $r = 0.89$ for Spearman, both *p-value* < 0.01). Thus, a statistically significant change

in the PC 1 of MAM NDVI anomalies is related to increased irrigation. Data for irrigated area are annual, so we cannot compare with the previous season, for example. The previous annual and simultaneous MAM rainfall in the Indian subcontinent are not significantly correlated with the MAM NDVI ($r = 0.28$ and 0.12, respectively, *p-value* > 0.1), indicating that irrigation expansion is more responsible for increased MAM NDVI than changes in precipitation. We take the standardized PC 1 of MAM NDVI anomalies as an index for vegetation change to examine the effects of land cover change on early ISM variability shown in the next section.

4. Effects of land cover change on early ISM variability

4.1. Trend and correlation analyses

July ISM rainfall significantly decreases on the central and southern Indian subcontinent and increases over the northern Bay of Bengal for 1982–2003 (Figure 2(a)). Decreased July rainfall occurs around 17°N and 77°E where MAM NDVI anomalies significantly increase (Figure 1(e)). In order to determine the relationship between land cover change during the preceding MAM and early ISM rainfall, we examine the spatial pattern

in the correlation between July rainfall and the PC 1 of MAM NDVI anomalies. July ISM rainfall is negatively correlated with the PC 1 of MAM NDVI anomalies in the central and southern Indian subcontinent, and is positively correlated with the PC 1 of MAM NDVI in the northern Bay of Bengal (Figure 2(b)). The spatial distribution of the correlation is similar to that of the regression trend in July rainfall shown in Figure 2(a). To check if significant correlations are due to the trends, July rainfall and the PC 1 of MAM NDVI anomalies are detrended. The detrended values still show a significant (*p*-value <0.1) negative correlation in the southern Indian subcontinent, though the significant positive correlation in the northern Bay of Bengal disappears (Figure 2(c)). After detrending, the centre of negative correlation is shifted to the east, because the strong correlation due to significant trends in both the MAM NDVI and July rainfall was removed for central-western India around 17°N and 77°E. The spatial correlation between Figure 2(b) and

(c) (144 data points) is 0.63, which is significant at the 99% level. The spatial patterns in Figure 2(a) and (b) are similar to non-parametric patterns based on the Spearman and Kendall's statistics (Figure 3). Thus, the trend and correlation analyses support the conclusion that the decrease in July ISM rainfall over the central and southern Indian subcontinent for 1982–2003 is significantly related to the increase in the preceding MAM NDVI anomalies.

4.2. Composite analysis

The difference between the mean July 200 hPa wind vector in the 5 years of highest PC 1 of MAM NDVI anomalies versus the mean wind vector in the 5 years of lowest PC 1 of MAM NDVI anomalies (i.e. composite difference) shows more westerly anomalies for the 5 years of highest NDVI (Figure 4(d)). The 22-year mean for 1982–2003 of upper level wind over India for July is easterly (Figure 4(a)), so these positive wind (westerly)
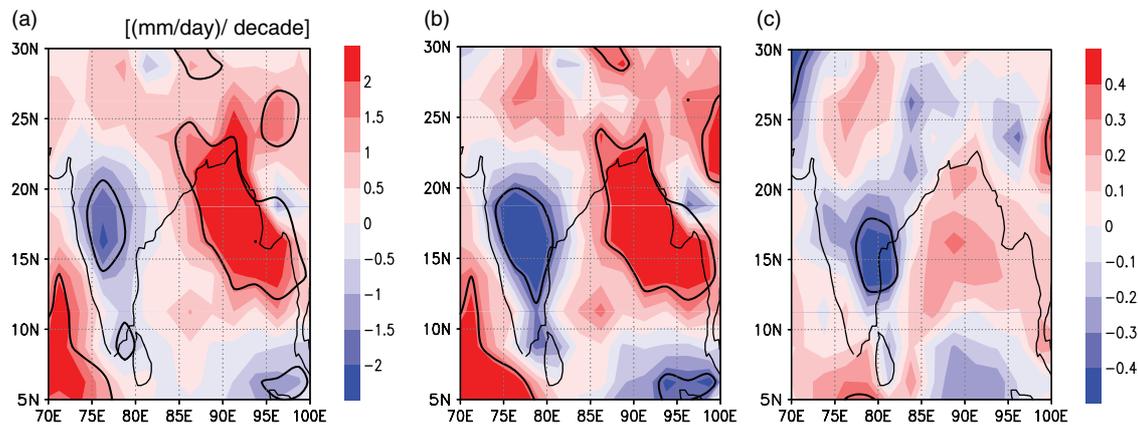

Figure 2. (a) Spatial distribution of 1982–2003 regression trend of July rainfall [(mm/day)/decade]. (b) Correlation patterns of July rainfall with the standardized PC 1 of MAM NDVI anomalies and (c) as in (b), but after detrending. Significant regions at the 90% level are contoured. This figure is available in colour online at www.interscience.wiley.com/ijoc
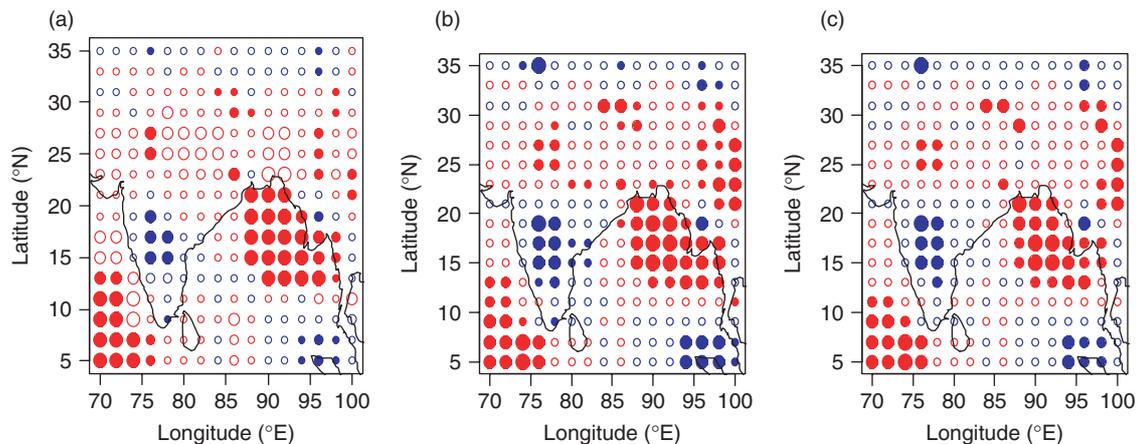

Figure 3. (a) Spatial distributions of 1982–2003 non-parametric regression trends of July rainfall, which is based on the Spearman rank correlation and Kendall–Theil methods. Red and blue circles indicate increasing and decreasing rainfall. The size of circle is proportional to the magnitude of trend. Circle size (from smallest to largest): <1, 1–1.5, 1.5–2, and >2 [(mm/day)/decade]. Correlation patterns of July rainfall with the standardized PC 1 of MAM NDVI anomalies using (b) Spearman and (c) Kendall correlations. Red and blue circles represent positive and negative correlations. The circle sizes correspond to <90, 90–95, 95–99, and >99% significance levels. In all figures, filled circles represent 90% significance level. This figure is available in colour online at www.interscience.wiley.com/ijoc
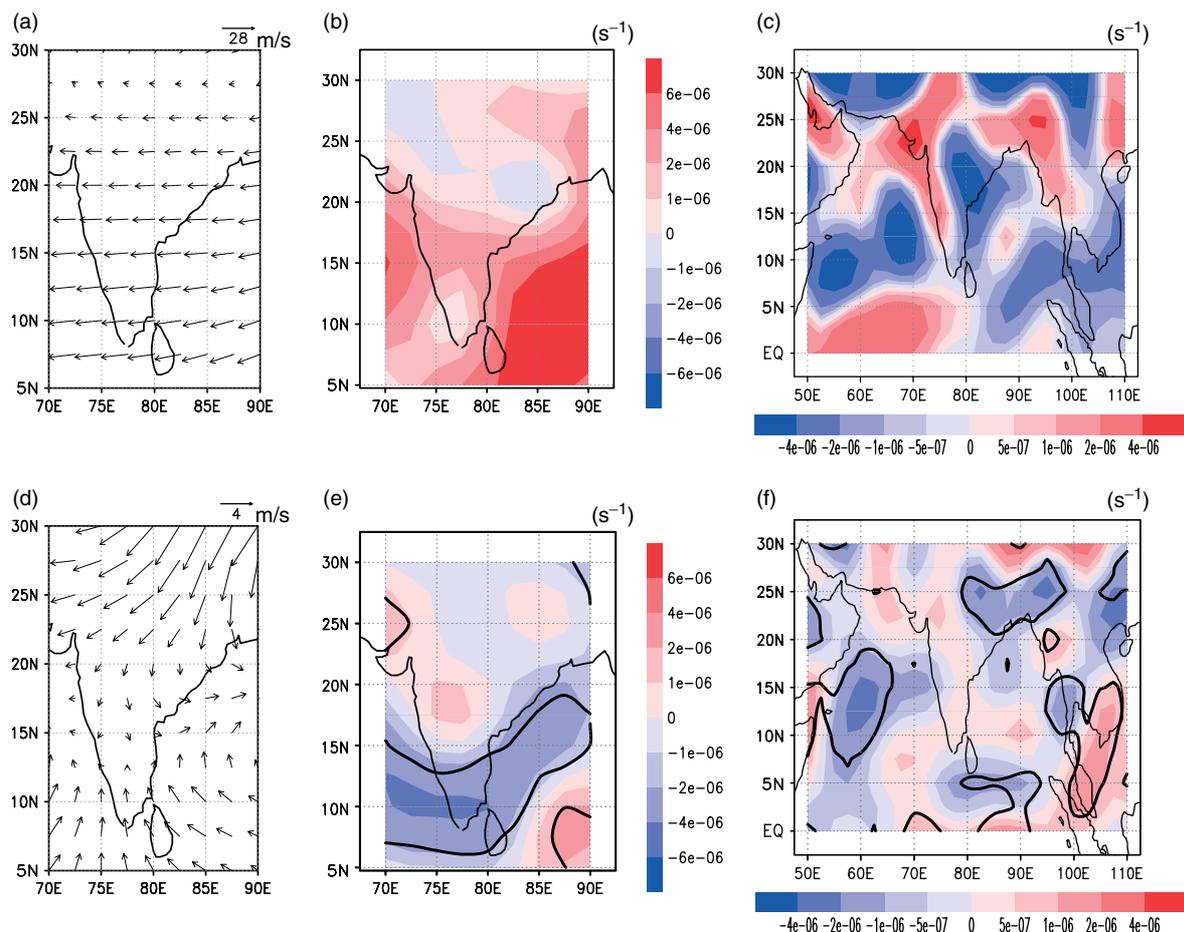
Figure 4. Twenty-two-year means (1982–2003) of (a) July 200 hPa wind vector (m/s), (b) July 200 hPa divergence (s^{-1}), and (c) July 850 hPa divergence (s^{-1}) and their composite differences (d), (e), and (f) between the 5 years of highest and lowest PC 1 of MAM NDVI anomalies over India. Significantly different regions at the 90% level are contoured in (e) and (f). Positive (red) and negative (blue) values represent divergences and convergences. This figure is available in colour online at www.interscience.wiley.com/ijoc

anomalies represent weaker easterly winds in the upper troposphere and, therefore, a weaker July ISM. The difference in the upper level divergence of the 5 lowest years of MAM NDVI PC 1 from the 5 highest years is negative over southern India (Figure 4(e)), which is a region of positive upper level divergence (Figure 4(b)). This finding also supports the interpretation of weakened Indian summer monsoonal circulations.

The composite difference of July 850 hPa divergence between the 5 years of highest and lowest PC 1 of MAM NDVI anomalies (Figure 4(f)) shows more divergence anomalies over the Indian subcontinent and more convergence anomalies in the surrounding oceans for the 5 years with the highest NDVI PC 1 anomalies, again supporting a weaker July ISM on the land and a stronger ISM on the ocean during years with high NDVI anomalies. The opposite sign of rainfall change over land and ocean (Figures 2(a) and 3(a)) is supported by the analysis of Prasad and Hayashi (2007), which demonstrated observationally that a weak monsoon was climatologically accompanied by stronger convection over adjacent oceans, consistent with our results. The anomalous lower level divergence in the Indian subcontinent prevents the advance of the intertropical convergence zone (ITCZ)

fully inland. Since the ITCZ is not drawn deeply inland, increased rainfall over the ocean is expected.

5. Physical mechanism

In India, the July LHF increases for 1982–1998 (Figure 5(a)), the period of increasing PC 1 of MAM NDVI anomalies in Figure 1(d), and is especially significant in western and southern India (note that the NDVI decreases after 1998 and the July LHF decreases correspondingly in central and southern India since 1998 (Figure 5(b)). The change of trend in the July LHF is consistent with that in the July SHF, which decreases for 1982–1998 (Figure 5(c)) and increases for 1999–2003 (Figure 5(d)). It is also consistent with the change of trend in net irrigated area, which increases for 1982–1998 and decreases over 1999–2003 (Figure 1(b)). Observed July surface temperature, which decreases in central and north-western India over 1982–1998 (Figure 5(e)), is also consistent with an increased LHF and a decreased SHF for the same period. Arora *et al*. (2005) observed a decreased surface temperature in central and northern India during the pre-monsoon and monsoon seasons using

the temperature data of 125 stations throughout India over 1941–1999, consistent with our results. For 1999–2003, the increase in July surface temperature (Figure 5(f)) is consistent with a decreased LHF and an increased SHF for the same period. These LHF trends are consistent with those of the SHF and surface temperature, indicating that an increased July LHF causes decreases in both the July SHF and surface temperature.

July surface temperature decreased over the land but increased over the ocean for 1982–1998, the period of increasing net irrigated area and the MAM NDVI

Figure 5. Spatial distributions of regression trends of July LHF [(W/m^2)/decade] for (a) 1982–1998 and (b) 1999–2003, July SHF [(W/m^2)/decade] for (c) 1982–1998 and (d) 1999–2003, and July surface temperature (°C/decade) for (e) 1982–1998 and (f) 1999–2003. In (e) and (f), trends are not reported unless >66% of the periods are available and grey areas signify missing data. Significant regions at the 90% level are contoured in (a), (b), (c), and (d). This figure is available in colour online at www.interscience.wiley.com/ijoc

(Figure 5(e)). These trends in surface temperature can cause a decrease in the heat contrast between land and sea, which plays an important role in controlling the monsoon. A decreased land–sea heat contrast is consistent with a weakened monsoon (e.g. Meehl, 1994). Thus, the decrease in early ISM rainfall over the Indian subcontinent appears partially related to the decreased land–sea heat contrast, which is a result of the increase in soil moisture and evapotranspiration due to irrigation and the related increase in the MAM NDVI, both of which correspond to an increase in the LHF (Figure 5(a)) and a decrease in the SHF (Figure 5(c)).

This study identifies statistical relationships among irrigation, NDVI, LHF, SHF, surface temperature, and early monsoon rainfall, and shows that there is a plausible line of physical processes linking these phenomena. Physical linkages proposed between irrigation and vegetation activity and early ISM rainfall are shown in Figure 6.

6. Conclusions

During 1982–2003, the net irrigated area for India significantly increased by 8628 km^2 per year due to numerous irrigation structures that were built as part of the green revolution. NDVI increased significantly for the same period with a very strong increase from 1982 to 1998 (decreasing slightly after 1998) during the pre-ISM season (MAM) over the Indian subcontinent. The MAM NDVI is strongly and significantly correlated with the net irrigated area ($r = 0.87$). Increased soil moisture, increased vegetation growth, and increased evapotranspiration would favour an increase in the LHF and a decrease in the SHF. For 1982–1998, the period of increasing net irrigation area and the MAM NDVI, July LHF in western and southern India significantly increased, and July SHF decreased. For 1982–2003, early ISM rainfall (July) significantly decreases on the central and southern Indian subcontinent. ISM rainfall in central and southern India is also significantly and negatively correlated with the PC 1 of the preceding MAM NDVI anomalies. Composite analyses of the 200 hPa wind vector and 200 and 850 hPa divergences show that the early ISM on the land is weaker for the years having
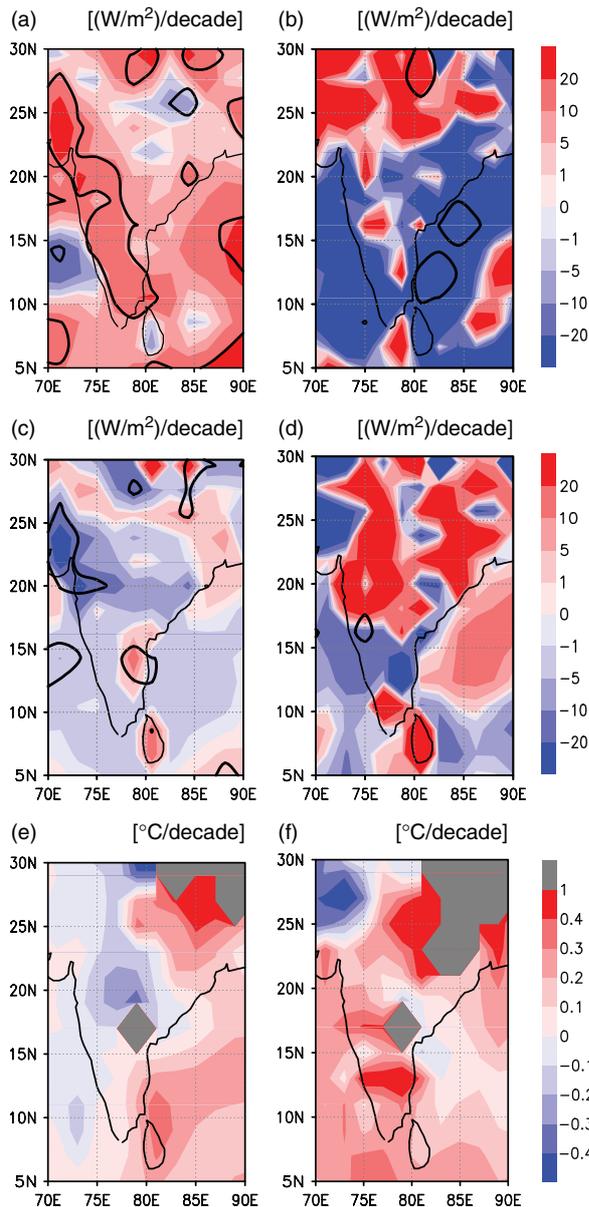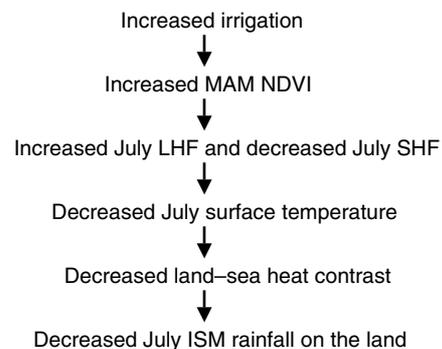

Figure 6. Physical linkages proposed between irrigation and vegetation activity and early ISM rainfall.

more vegetation activity during the pre-ISM season. We show that more July 850 hPa divergence anomalies in the Indian subcontinent for the years of highest MAM NDVIs prevent the advance of the ITCZ fully inland, and increased rainfall (more July 850 hPa convergence anomalies) over the surrounding oceans is expected.

We give evidence for a decreased land–sea heat contrast due to a decreased surface temperature resulting from an increased LHF, which appears to dominate any increased instability due to increased atmospheric moisture. This study supports the conclusion that the weak early ISM is due to the increase in irrigated area and the related increase in vegetation activity during the pre-ISM season, which promotes an increase in LHF and a decrease in SHF thereby favouring a reduced horizontal temperature gradient. Therefore, irrigation and vegetation activity appear to be a significant factor affecting the ISM. Other factors such as the phase of El Niño/Southern Oscillation (e.g. Kumar *et al.*, 2006) or atmospheric aerosols (e.g. Ramanathan *et al.*, 2001; Sarkar and Kafatos, 2004) also likely play roles that were not included in our study. We used surface heat fluxes from reanalysis data, which confirm the plausibility of the mechanism proposed in Section 5. Completely establishing the physical chain of events will require more detailed observations of surface heat fluxes.

Acknowledgements

References

Adler RF, Huffman GJ, Chang A, Ferraro R, Xie P-P, Janowiak J, Rudolf B, Schneider U, Curtis S, Bolvin D, Gruber A, Susskind J, Arkin P, Nelkin E. 2003. The version-2 global precipitation climatology project (GPCP) monthly precipitation analysis (1979–present). *Journal of Hydrometeorology* **4**: 1147–1167.

Anyamba A, Eastman JR. 1996. Interannual variability of NDVI over Africa and its relation to El Niño Southern oscillation. *International Journal of Remote Sensing* **17**: 2533–2548.

Arora M, Goel NK, Singh P. 2005. Evaluation of temperature trends over India. *Hydrological Sciences Journal-Journal Des Sciences Hydrologiques* **50**: 81–93.

Biggs TW, Thenkabail PS, Gumma MK, Scott C, Parthasaradhi GR, Turral H. 2006. Irrigated area mapping in heterogeneous landscapes with MODIS time series, ground truth and census data, Krishna Basin, India. *International Journal of Remote Sensing* **27**: 4245–4266.

Center for Monitoring Indian Economy. 2006. *Agriculture*. Center for Monitoring Indian Economy: Mumbai.

Chase TN, Knaff JA, Pielke RA, Kalnay E. 2003. Changes in global monsoon circulations since 1950. *Natural Hazards* **29**: 229–254.

Chase TN, Pielke RA Sr, Kittel TGF, Baron JS, Stohlgren TJ. 1999. Potential impacts on Colorado Rocky Mountain weather due to land use changes on the adjacent Great Plains. *Journal of Geophysical Research* **104**: 16 673–16 690.

Chase TN, Pielke RA Sr, Kittel TGF, Nemani RR, Running SW. 2000. Simulated impacts of historical land cover changes on global climate in northern winter. *Climate Dynamics* **16**: 93–105.

Cihlar J, St. Laurent L, Dyer JA. 1991. The relation between normalized difference vegetation index and ecological variables. *Remote Sensing of Environment* **35**: 279–298.

de Rosnay P, Polcher J, Laval K, Sabre M. 2003. Integrated parameterization of irrigation in the land surface model ORCHIDEE. Validation over Indian Peninsula. *Geophysical Research Letters* **30**(19): 1986, DOI:10.1029/2003GL018024.

Douglas EM, Niyogi D, Frolking S, Yeluripati JB, Pielke RA Sr, Niyogi N, Vörösmarty CJ, Mohanty UC. 2006. Changes in moisture and energy fluxes due to agricultural land use and irrigation in the Indian Monsoon Belt. *Geophysical Research Letters* **33**: L14403, DOI:10.1029/2006GL026550.

Foley JA, Costa MH, Delire C, Ramankutty N, Snyder P. 2003. Green Surprise? How terrestrial ecosystems could affect earth's climate. *Frontiers in Ecology and the Environment* **1**: 38–44.

Government of India. 1981–2003. *Indian Agricultural Statistics*. Ministry of Agriculture, Government of India: New Delhi.

Grantz K, Rajagopalan B, Clark M, Zagona E. 2007. Seasonal shifts in the North American monsoon. *Journal of Climate* **20**: 1923–1935.

Gray TI, Tapley DB. 1985. Vegetation health: nature's climate monitor. *Advances in Space Research* **5**: 371–377.

Hansen J, Lebedeff S. 1987. Global trends of measured surface air temperature. *Journal of Geophysical Research* **92**(D11): 13 345–13 372.

Hansen J, Ruedy R, Glascoe J, Sato M. 1999. GISS analysis of surface temperature change. *Journal of Geophysical Research* **104**: 30997–31022, DOI:10.1029/1999JD900835.

Ichii K, Kawabata A, Yamaguchi Y. 2002. Global correlation analysis for NDVI and climate variables and NDVI trends: 1982–1990. *International Journal of Remote Sensing* **23**: 3873–3878.

Justice CO, Townshend JRG, Holben BN, Tucker CJ. 1985. Analysis of the phenology of global vegetation using meteorological satellite data. *International Journal of Remote Sensing* **6**: 1271–1318.

Kalnay E, Kanamitsu M, Kistler R, Collins W, Deaven D, Gandin L, Iredell M, Saha S, White G, Woollen J, Zhu Y, Chelliah M, Ebisuzaki W, Higgins W, Janowiak J, Mo KC, Ropelewski C, Wang J, Leetmaa A, Reynolds R, Jenne R, Joseph D. 1996. The NCEP/NCAR 40-year reanalysis project. *Bulletin of the American Meteorological Society* **77**: 437–471.

Kanamitsu M, Ebisuzaki W, Woollen J, Yang S-K, Hnilo JJ, Fiorino M, Potter GL. 2002. NCEP-DOE AMIP-II reanalysis (R-2). *Bulletin of the American Meteorological Society* **83**: 1631–1643.

Kawabata A, Ichii K, Yamaguchi Y. 2001. Global monitoring of interannual changes in vegetation activities using NDVI and its relationships to temperature and precipitation. *International Journal of Remote Sensing* **22**: 1377–1382.

Kumar KK, Rajagopalan B, Hoerling M, Bates G, Cane M. 2006. Unraveling the mystery of Indian monsoon failure during El Niño. *Science* **314**: 115–119.

Lawrence PJ, Chase TN. Climate Impacts of making the hydrology of the Community Land Model (CLM 3.0) consistent with the Simple Biosphere Model (SiB 2.0). *Journal of Hydrometeorology* (in press).

Leavitt SW, Chase TN, Rajagopalan B, Lee E, Lawrence PJ. Southwestern U.S. tree-ring carbon isotope indices as a possible proxy for reconstruction of greenness of vegetation. *Geophysical Research Letters* (in press).

Lee E, Chase TN, Rajagopalan B. 2008. Seasonal forecasting of East Asian summer monsoon based on oceanic heat sources. *International Journal of Climatology* **28**: 667–678.

Li Z, Kafatos M. 2000. Interannual variability of vegetation in the United States and its relation to El Niño/Southern Oscillation. *Remote Sensing of Environment* **71**: 239–247.

Lohar D, Pal B. 1995. The effect of irrigation on premonsoon season precipitation over South West Bengal, India. *Journal of Climate* **8**: 2567–2570.

Meehl GA. 1994. Influence of the land surface in the Asian summer monsoon: External conditions versus internal feedback. *Journal of Climate* **7**: 1033–1049.

Myneni RB, Hall FG, Sellers PJ, Marshak AL. 1995. The interpretation of spectral vegetation indexes. *IEEE Transactions on Geoscience and Remote Sensing* **33**: 481–486.

Pielke RA Sr, Marland G, Betts R, Chase TN, Eastman JL, Niles JO, Niyogi D, Running SW. 2002. The influence of land-use change and landscape dynamics on the climate system: relevance to climate-change policy beyond the radiative effect of greenhouse gasses. *Philosophical Transactions of the Royal Society of London Series A-Mathematical Physical and Engineering Sciences* **360**: 1705–1719.

Prasad VS, Hayashi T. 2007. Active, weak and break spells in the Indian summer monsoon. *Meteorology and Atmospheric Physics* **95**: 53–61.

Ramanathan V, Crutzen PJ, Kiehl JT, Rosenfeld D. 2001. Aerosols, climate, and the hydrological cycle. *Science* **294**: 2119–2124.

Sarkar S, Kafatos M. 2004. Interannual variability of vegetation over the Indian sub-continent and its relation to the different meteorological parameters. *Remote Sensing of Environment* **90**: 268–280.

Shiklomanov IA (Ed.). 1997. *Assessment of Water Resources and Water Availability in the World*. World Meteorological Organization/Stockholm Environment Institute: Geneva, Switzerland, 88.

Siebert S, Doll P, Hoogeveen J, Faures J-M, Frenken K, Feick S. 2005. Development and validation of the global map of irrigation areas. *Hydrology and Earth System Sciences* **9**: 535–547.

Sud YC, Fennessy MJ. 1982. A study of the influence of surface albedo on July circulation in semi-arid regions using the GLAS GCM. *Journal of Climatology* **22**: 105–125.

Sud YC, Fennessy MJ. 1984. Influence of evaporation in semi-arid regions on the July circulation: a numerical study. *Journal of Climatology* **4**: 383–398.

Sud YC, Smith WE. 1985. Influence of local land-surface processes on the Indian Monsoon: a numerical study. *Journal of Climate and Applied Meteorology* **24**: 1015–1036.

Thenkabail P, Parthasaradhi G, Biggs TW, Gumma MK, Turral H. 2007. Spectral matching techniques to determine historical land use/land cover (LULC) and irrigated areas using time-series AVHRR Pathfinder datasets in the Krishna river basin, India. *Photogrammetric Engineering and Remote Sensing* **73**: 1029–1040.

Tomita T, Sato H, Nonaka M, Hara M. 2007. Interdecadal variability of the early summer surface heat flux in the Kuroshio region and its impact on the Baiu frontal activity. *Geophysical Research Letters* **34**: L10708, DOI:10.1029/2007GL029676.

Tucker CJ, Pinzon JE, Brown ME, Slayback DA, Pak EW, Mahoney R, Vermote EF, Saleous N. 2005. An extended AVHRR 8-km NDVI dataset compatible with MODIS and SPOT vegetation NDVI data. *International Journal of Remote Sensing* **26**: 4485–4498.

von Storch H, Zorita E, Jones JM, Dimitriev Y, González-Rouco F, Tett SFB. 2004. Reconstructing past climate from noisy data. *Science* **306**: 679–682.

von Storch H, Zwiers FW. 2001. *Statistical Analysis in Climate Research*. Cambridge University Press: Cambridge.

Wang B, Ding Q. 2006. Changes in global monsoon precipitation over the past 56 years. *Geophysical Research Letters* **33**: L06711, DOI:10.1029/2005GL025347.

Wang B, Wu R, Fu X. 2000. Pacific-East Asian teleconnection: how does ENSO affect East Asian climate? *Journal of Climate* **13**: 1517–1536.